

# CLINICAL INSPIRED MRI LESION SEGMENTATION

Lijun Yan\*

Churan Wang<sup>†</sup>✉

Fangwei Zhong<sup>‡</sup>

Yizhou Wang<sup>†</sup>

✉ Correspondence to: [churanwang@pku.edu.cn](mailto:churanwang@pku.edu.cn)

\*School of Software and Microelectronics, Peking University, China.

<sup>†</sup>Center on Frontiers of Computing Studies, School of Computer Science, Nat'l Eng. Research Center of Visual Technology, Peking University, China.

<sup>‡</sup>School of Artificial Intelligence, Beijing Normal University, China.

## ABSTRACT

Magnetic resonance imaging (MRI) is a potent diagnostic tool for detecting pathological tissues in various diseases. Different MRI sequences have different contrast mechanisms and sensitivities for different types of lesions, which pose challenges to accurate and consistent lesion segmentation. In clinical practice, radiologists commonly use the sub-sequence feature, i.e. the difference between post contrast-enhanced T1-weighted (post) and pre-contrast-enhanced (pre) sequences, to locate lesions. Inspired by this, we propose a residual fusion method to learn subsequence representation for MRI lesion segmentation. Specifically, we iteratively and adaptively fuse features from pre- and post-contrast sequences at multiple resolutions, using dynamic weights to achieve optimal fusion and address diverse lesion enhancement patterns. Our method achieves state-of-the-art performances on BraTS2023 dataset for brain tumor segmentation and our in-house breast MRI dataset for breast lesion segmentation. Our method is clinically inspired and has the potential to facilitate lesion segmentation in various applications.

**Index Terms**— Tumor Segmentation, CE MRI

## 1. INTRODUCTION

Magnetic Resonance Imaging (MRI), a non-invasive and radiation-free 3D medical imaging technique, plays a crucial role in screening [1], diagnosing, and treating various diseases due to its high sensitivity and detailed anatomical visualization. The initial MRI scanning involves T1-weighted sequences, known as pre-contrast sequences. Then, a contrast agent, typically Gadolinium (Gd), is administered, followed by multiple scans of T1 sequences, creating post-contrast sequences [2]. Post-contrast sequences highlight structures like blood vessels, inflammation, and lesions with elevated signal intensity. Comparing pre-contrast and post-contrast sequences enables doctors to identify potential lesions.

Distinct enhancement patterns are observed in different tissues [3, 4]. Tissues with abundant blood supply, such as tumors and inflammation, often exhibit high signal intensity in enhanced images. Conversely, structures like cysts

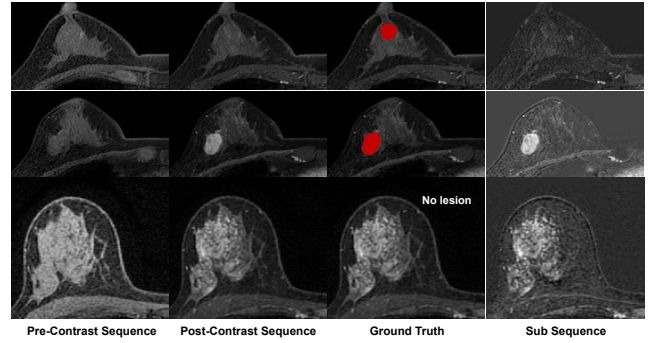


**Fig. 1.** Overview of enhancement patterns. The four columns represent pre-contrast images, post-contrast images, the lesions drawn by radiologists, and the subtraction images (SUB). The three rows represent fibroadenoma, typical mass, and well-vascularized glandular tissue respectively.

and calcification show no enhancement. Furthermore, certain healthy tissues may undergo enhancement; for instance, normal breast fibroglandular tissue may appear highly enhanced in post-contrast sequence due to its rich blood supply (Fig. 1 illustrates these scenarios). Given the diversity in enhancement patterns, clinical diagnosis requires radiologists to analyze both pre-contrast and post-contrast sequences, because depending solely on post-contrast sequences for diagnosis is one-sided and error-prone and a comprehensive diagnosis must integrate pre-contrast information.

An intuitive idea to achieve the fusion of pre-contrast and post-contrast MRI sequences is to directly utilize pre-contrast and post-contrast images and design attention-based mechanisms [5, 6, 7, 8, 9, 10, 11]. Meanwhile, some methods focus on learning the enhancement process and extracting corresponding lesion information [12, 13]. However, direct fusion approaches may not fully utilize the distinct and complementary information each sequence offers. Moreover, they may not adequately address the variations in image characteristics, such as noise levels and contrast differences, potentially impacting the accuracy of lesion characterization.

To solve this problem, we focus on how to naturally explore the relationship between pre-contrast and post-contrast

images. The residual concept aligns more closely with the diagnostic process, where radiologists often look for changes between sequences to make informed decisions. Inspired by residual learning [14] and counterfactual generation[15, 16], we propose a residual learning framework. Our approach focuses on learning the differences or ‘residuals’ between pre-contrast and post-contrast images. We involve integrating pre-contrast images into the segmentation encoder at each encoding step, enabling the network to focus on learning enhancement patterns. By doing so, our network can more effectively highlight the changes due to contrast enhancement, which is critical for accurate lesion detection and segmentation. Hence, our method not only improves the integration of MRI sequences but also enhances the clinical relevance of the segmentation results. In general, our work contributes in the following ways:

- We introduce a novel neural network architecture that seamlessly incorporates pre-contrast information into post-contrast images, contributing to enhanced lesion diagnosis and segmentation, with only a minimal increase in the parameters of the backbone network.
- Aligning with the diagnostic practices of radiologists, our method leverages more comprehensive information, enhancing lesion diagnosis and segmentation efficacy.
- Our model achieves state-of-the-art performance in brain tumor and breast lesion segmentation tasks.

## 2. METHOD

Our study proposes a model integrating pre- and post-contrast T1-weighted images to enhance tumor analysis, with the network architecture shown in Fig. 2. We extract features from both images using shared neural networks in encoding blocks, capturing local and global features via convolutional architectures. Post-T1 images, with enhanced brightness for lesions, form the main branch, while pre-T1 images serve as an auxiliary branch. Additionally, a multi-scale feature fusion mechanism is implemented to learn residuals of image features at various scales, enabling the model to grasp intricate details across scales and improve lesion exploration performance.

### 2.1. Residual Module & Multi-scale Feature Aggregation

Derived from the ResNet architecture [14], we incorporate skip connections into the encoding process, departing from the traditional Res-UNet [17] approach where input features directly link to post-convolutional features. Our innovation involves residual learning of the main branch and the auxiliary branch, fostering a feature fusion step between the main and auxiliary branches.

Inspired by residual learning in ResNet, we propose a method to learn the residual between two branches. Fig. 2 illustrates the residual module in ResNet and the modified residual module we derived. Fig. 2(a) shows the original residual module from the ResNet paper, which improves training efficiency and stability by learning the difference

**Table 1.** Comparison among recent methods on our in-house breast MRI dataset.

| Methodology    | DSC           | Recall        |
|----------------|---------------|---------------|
| ResUNet[17]    | 78.10%        | 74.47%        |
| A2FNet[6]      | 80.01%        | 79.54%        |
| TSF-Seq2Seq[7] | 80.22%        | 80.63%        |
| LiTS[8]        | 79.99%        | 79.50%        |
| Ours           | <b>82.55%</b> | <b>82.05%</b> |

(i.e. residual  $F(x)$ ) between the input  $x$  and the desired output  $H(x)$ . Considering that the MRI images before and after enhancement theoretically only have significant differences in the lesion areas and have very similar structures, we modify the residual module, which is shown in Fig. 2(b). We set the desired output as  $H(x) = E(x_{main}) + x_{aux}$ , which enables the network to more efficiently learn lesion-related features through the residuals between the two branches.

Throughout the multiple down-sampling stages of the encoder-decoder architecture, we repeatedly use the modified residual module mentioned above, ensuring the integration of both the main and auxiliary branches across different resolutions. This approach aims to enhance the network’s capacity to capture intricate details and contextual information at diverse levels. By linking feature maps from the auxiliary branch to the main branch, our model can leverage both the detailed information learned by the main branch and the contrasting information provided by the auxiliary branch.

This feature fusion strategy not only maintains the network’s high-resolution information capture capability but also enriches feature representations with complementary details from both branches. The resulting network architecture is well-suited for medical image analysis tasks, particularly in scenarios where accurate diagnosis and segmentation require the incorporation of intricate details and subtle contrasts.

### 2.2. Dynamic Learning of Auxiliary Branch Weights

The fusion of features from both branches involves a direct addition operation. However, recognizing the need for different weights for features of the two branches, we introduce a block designed to dynamically learn the weights of the auxiliary branch before the addition operation. Specifically, we employ a  $1*1*1$  convolutional layer to dynamically learn these weights. The schematic of the final residual module is shown in Fig. 2(c). This approach introduces a minimal number of parameters, ensuring efficiency, while also allowing for adaptable weight adjustments for the auxiliary branch.

## 3. EXPERIMENTS

### 3.1. Dataset

**In-house Breast Dataset:** The breast MRI dataset encompasses a total of 515 cases. The dataset comprises images acquired from Siemens, GE, and Philips MRI machines, featuring both pre-contrast and post-contrast T1-weighted se-

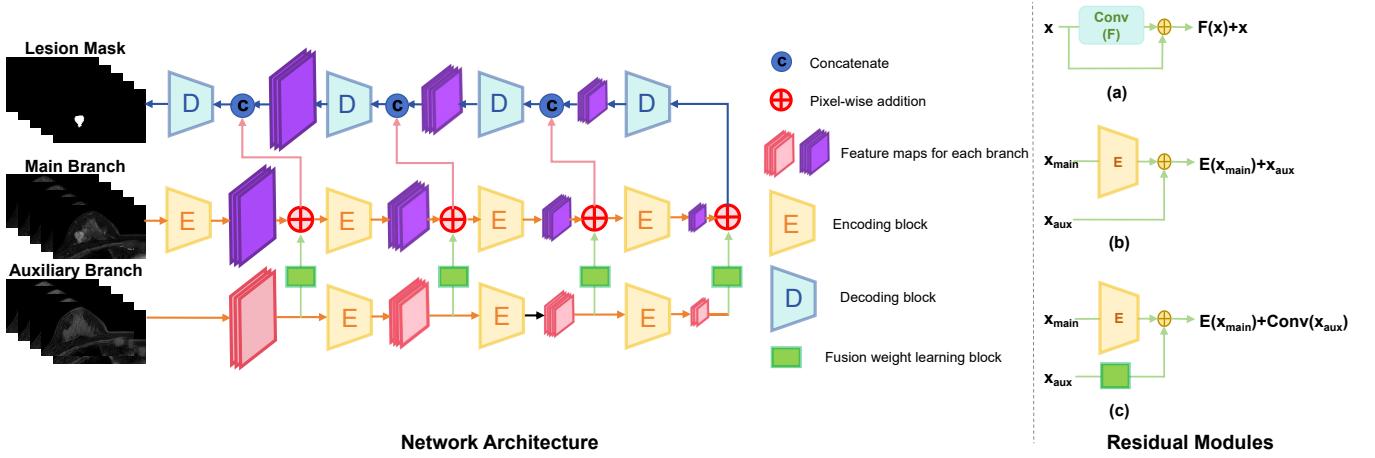


**Fig. 2.** **Left:** The architecture of our network, featuring a main branch and an auxiliary branch, each comprising encoding blocks, as well as fusion weight learning blocks. **Right:** residual modules of different versions. (a) is the original version from ResNet, (b) is our modified version which incorporates two branches, and (c) is our final residual module which adds a fusion weight learning block into (b).

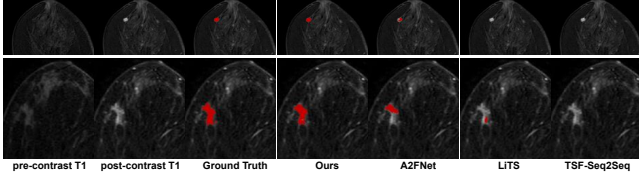


**Fig. 3.** Visualization of breast lesion segmentation. Each row represents a case from our in-house dataset.

quences. Experienced radiologists annotated lesion masks for each case in our dataset, ensuring high-quality ground truth.

**BraTS2023 Glioma:** The BraTS2023 Glioma dataset includes 1126 cases. This comprehensive dataset incorporates T1-weighted and post-contrast T1-weighted sequences. The dataset also provides segmentation masks for tumors.

### 3.2. Experimental Results

Our proposed module can adapt to various encoders and decoders. To maintain comparability with ResUNet, we used encoders from ResUNet architecture in our experiments, consistent with that in [17].

To assess the effectiveness of our proposed method, we conduct comparative experiments with three recent papers: A2FNet [6], TSF-Seq2Seq [7] and LiTS [8]. We also conduct experiments solely on post-contrast images, denoted as Res-UNet-Single. We utilize Dice Coefficient (DSC) and recall (at pixel level) as evaluation metrics

**In-house Breast Dataset:** Experimental results on our in-house breast MRI dataset are presented in Tab. 1. Our proposed approach achieves DSC of 82.55%, surpassing the performance of all compared methodologies. Additionally, the Recall for our method stands at 82.05%, demonstrating its effectiveness in accurately capturing relevant information within the breast MRI dataset. The results underscore the superior performance of our proposed method in comparison to state-of-the-art techniques, highlighting its potential for

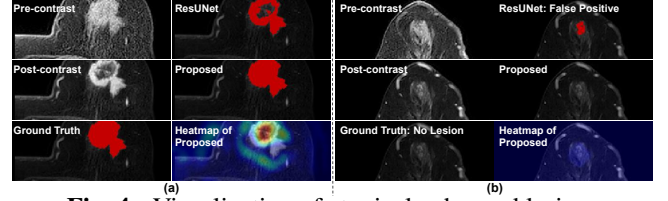


**Fig. 4.** Visualization of atypical enhanced lesion.

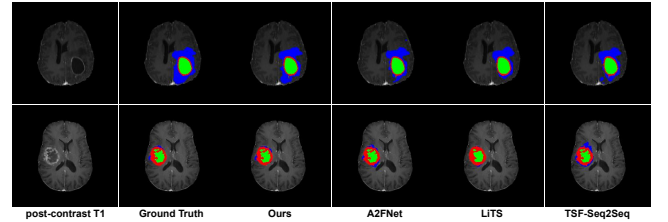


**Fig. 5.** Visualization of brain tumor segmentation. Each row shows a case from the BraTS2023 dataset. WT=red+green+blue; TC=red+green; EN=red.

robust and accurate segmentation in breast MRI applications.

Fig. 3 shows the segmentation results of different models on breast MRI, each row represents a patient with a lesion segmented out by radiologists. The lesion in the first row is a very small, spot-like enhancement that some models tend to overlook, our model maintains a high detection rate for small lesions. The lesion in the second patient has an irregular shape with additional spot-like local enhancements. Only our model can fully detect the irregular contour of the entire lesion.

We also select two visualization results to further demonstrate the function of the aux-branch, which is shown in Fig. 4. The lesion from patient (a) exhibits significant heterogeneous enhancement after contrast, with the central area being a low-enhancement zone. The second column shows the segmentation results of ResUNet and our proposed model, respectively, which shows that incorporating the pre-contrast phase signif-

**Table 2.** Comparison among recent methods on BraTS2023 dataset. WT=whole tumor, TC=tumor core, EN=enhancing.

| Methodology    | DSC           |               |               |               |
|----------------|---------------|---------------|---------------|---------------|
|                | WT            | TC            | EN            | Mean          |
| ResUNet[17]    | 76.74%        | 86.60%        | 83.52%        | 82.29%        |
| A2FNet[6]      | 80.96%        | 87.98%        | 84.20%        | 84.38%        |
| TSF-Seq2Seq[7] | 80.87%        | 87.83%        | 85.73%        | 84.81%        |
| LiTS[8]        | 81.03%        | 88.34%        | 83.37%        | 84.25%        |
| Ours           | <b>83.87%</b> | <b>89.17%</b> | <b>86.28%</b> | <b>86.44%</b> |

icantly improves the segmentation of the low-contrast area. The bottom right image illustrates the heatmap, demonstrating that our model accurately identifies areas that require attention. Meanwhile, patient (b) is a classic case of glandular enhancement. The ResUNet model’s prediction, which does not incorporate pre-contrast information, includes false positives. In contrast, our model mitigates the occurrence of false positives and achieves better performance.

**BraTS2023 Glioma Dataset:** Tab. 2 shows DSC values for Whole Tumor (WT), Tumor Core (TC), and Enhancing (EN) regions on the BraTS2023 Glioma dataset. Our method achieves the highest DSCs: 83.87% for WT, 89.17% for TC, and 86.28% for EN, with an overall mean of 86.44%. This consistent superiority shows the effectiveness of our approach and its potential for accurate glioma segmentation in clinical settings. Fig. 5 shows brain MRI segmentation results from different models. Accurate boundary delineation between brain tissue and lesion areas, particularly the challenging tumor edema region (blue in the figure), is crucial. Our model outperforms others by providing clearer edema boundaries while maintaining high core tumor segmentation accuracy.

#### 4. CONCLUSION

Inspired by the clinical diagnostic practices of radiologists, we introduce a new method that combines data from both pre- and post-contrast MRI scans. This innovative approach is characterized by its multi-scale fusion of images, which is adeptly modulated by dynamically adjusted fusion weights. This method is pivotal as it enriches the model’s ability to delineate lesion boundaries with heightened precision and to discern subtle abnormalities with greater clarity. Despite not causing a substantial rise in the parameter count, experiments conducted on both our in-house breast and the BraTS2023 Glioma dataset show the superior performance of this network in segmentation tasks. Moreover, our method stands out as a clinically inspired solution, promising to elevate the standards of MRI lesion segmentation in line with the real-world demands of medical diagnostics.

#### Acknowledgments

This work was supported by the State Key Lab of General Artificial Intelligence at Peking University and Qualcomm University Research Grant.

#### 5. REFERENCES

- [1] E. Morris, C. Comstock, C. Lee *et al.*, *ACR BI-RADS Magnetic Resonance Imaging*. American College of Radiology, 2013.
- [2] H. Bougias and N. Stogiannos, “Breast mri: Where are we currently standing?” in *Journal of Medical Imaging and Radiation Sciences*, vol. 53, no. 2, June 2022, pp. 203–211.
- [3] R. M. Mann, N. Cho, and L. Moy, “Breast mri: State of the art.” in *Radiology*, vol. 292, no. 3, December 2019, pp. 520–536.
- [4] J. G. Smirniotopoulos, F. M. Murphy, E. J. Rushing, J. H. Rees, and J. W. Schroeder, “Patterns of contrast enhancement in the brain and meninges.” in *Radiographics*, vol. 27, no. 2, March–April 2007, pp. 525–551.
- [5] A. Galli, S. Marrone, G. Piantadosi, M. Sansone, and C. Sansone, “A pipelined tracer-aware approach for lesion segmentation in breast dce-mri.” in *Journal of Imaging*, vol. 7, no. 12, December 2021, pp. 1–11.
- [6] Z. Wang and Y. Hong, “A2fseg: Adaptive multi-modal fusion network for medical image segmentation,” in *MICCAI*, vol. 14223. Cham: Springer, 2023, pp. 64–70.
- [7] L. Han *et al.*, “An explainable deep framework: Towards task-specific fusion for multi-to-one mri synthesis,” in *MICCAI*, vol. 14229. Cham: Springer, 2023, pp. 5–11.
- [8] Y. Zhang, C. Peng, R. Tong, L. Lin, Y. Chen, Q. Chen *et al.*, “Multi-modal tumor segmentation with deformable aggregation and uncertain region inpainting,” *IEEE Trans. Med. Imag.*, vol. 42, no. 10, pp. 3091–3103, October 2023.
- [9] S. Wang, K. Sun, L. Wang, L. Qu, F. Yan, Q. Wang *et al.*, “Breast tumor segmentation in dce-mri with tumor sensitive synthesis,” *IEEE Trans. Neural Netw. Learn. Syst.*, vol. 34, no. 8, pp. 4990–5001, August 2023.
- [10] A. Hatamizadeh *et al.*, “Unetr: Transformers for 3d medical image segmentation,” in *WACV*. IEEE, 2022, pp. 1748–1758.
- [11] A. Rahman, J. M. J. Valanarasu, I. Hacihaliloglu, and V. M. Patel, “Ambiguous medical image segmentation using diffusion models,” in *CVPR*. IEEE, 2023, pp. 11 536–11 546.
- [12] T. Lv, Y. Liu, K. Miao, L. Li, and X. Pan, “Diffusion kinetic model for breast cancer segmentation in incomplete dce-mri,” in *MICCAI*, vol. 14223. Cham: Springer, 2023, pp. 10–16.
- [13] M. Chung, E. Calabrese, J. Mongan, K. M. Ray, J. H. Hayward, T. Kelil *et al.*, “Deep learning to simulate contrast-enhanced breast mri of invasive breast cancer,” *Radiology*, vol. 306, no. 3, p. E213199, 2023.
- [14] K. He, X. Zhang, S. Ren, and J. Sun, “Deep residual learning for image recognition,” in *CVPR*. IEEE, 2016, pp. 770–778.
- [15] C. Wang, F. Zhang, Y. Yu, and Y. Wang, “Br-gan: Bilateral residual generating adversarial network for mammogram classification,” in *MICCAI*, vol. 12262. Cham: Springer, 2020, pp. 10–16.
- [16] C. Wang, J. Li, F. Zhang *et al.*, “Bilateral asymmetry guided counterfactual generating network for mammogram classification,” *IEEE Trans. Image Process.*, vol. 30, pp. 7980–7994, 2021.
- [17] Z. Zhang, Q. Liu, and Y. Wang, “Road extraction by deep residual u-net,” *IEEE Geosci. Remote Sens. Lett.*, vol. 15, no. 5, pp. 749–753, May 2018.